
Multi-Agent Reinforcement Learning Guided by Signal Temporal Logic Specifications

Jiangwei Wang

University of Connecticut

Shuo Yang

University of Pennsylvania

Ziyan An

Vanderbilt University

Songyang Han

University of Connecticut

Zhili Zhang

University of Connecticut

Rahul Mangharam

University of Pennsylvania

Meiyi Ma

Vanderbilt University

Fei Miao

University of Connecticut

Abstract

There has been growing interest in deep reinforcement learning (DRL) algorithm design, and reward design is one key component of DRL. Among the various techniques, formal methods integrated with DRL have garnered considerable attention due to their expressiveness and ability to define the requirements for the states and actions of the agent. However, the literature of Signal Temporal Logic (STL) in guiding multi-agent reinforcement learning (MARL) reward design remains limited. In this paper, we propose a novel STL-guided multi-agent reinforcement learning algorithm. The STL specifications are designed to include both task specifications according to the objective of each agent and safety specifications, and the robustness values of the STL specifications are leveraged to generate rewards. We validate the advantages of our method through empirical studies. The experimental results demonstrate significant performance improvements compared to MARL without STL guidance, along with a remarkable increase in the overall safety rate of the multi-agent systems.

1 Introduction

Reinforcement learning (RL) and multi-agent reinforcement learning (MARL) have gained significant research interests in solving various sequential decision-making problems in recent years, especially with the rapid development of deep reinforcement learning (DRL). It has been widely adopted in various domains such as robotics, healthcare systems, autonomous driving, smart cities and others that involve the participation of more than one single agent and naturally fall into the realm of MARL [1]. It is a key component of an MARL algorithm to define a reward function that maps each state and an action that can be taken in that state to some real-valued reward [2]. However, designing a reward function that informally capture the desired behavior and objective of the agent considering the dynamic interactions among multi-agents remains challenging and an open question. In particular, for multi-agent systems with decision-making problems that involve both the interactions of the agents and the physical dynamic process of each individual agent, poorly designed reward functions can lead to undesired policies that are unable to accomplish the tasks, or worse, execute unsafe actions in safety-critical systems [3, 4].

A *motivating example* of decision-making for multi-agent system is shown in Fig. 1, where we consider lane merging decisions for a group of autonomous vehicles. In this case, the two red broken-down vehicles stopped on streets and blocked two lanes (due to an accident or other reasons), the three blue autonomous vehicles want to drive forward and pass through the only open lane (left lane in the figure) as soon as possible and keep a safety distance between each other and the broken-down vehicles. Hence, each agent should maintain a safety distance to the surrounding vehicles when

merging lane. Additionally, the duration during which autonomous vehicles remain blocked after the broken-down vehicles is also a concern. To expedite their arrival at their destinations, this duration should be kept below a certain threshold. In order to make the vehicles learn to fulfill all these requirements, designing a reward function may take lots of trials and can be quite time-consuming.

To address this challenge, we propose a safe multi-agent reinforcement learning algorithm that leverages signal temporal logic (STL) specifications and we use their robustness values as the reward. While there are extensive works exploring the use of temporal logic in single-agent RL, little attention has been drawn on how to design it to guide MARL [5, 6]. Given the complex interactions and typically heterogeneous goals among agents, designing rewards that enable agents to learn to solve the desired tasks becomes even more challenging. Furthermore, ensuring agents’ safety is crucial in safety-critical systems such as autonomous driving. Signal temporal logic (STL) as a formal language provides a more principled and expressive way to encode these requirements into STL specifications, and we adopt the robustness values based on the STL requirements in our proposed STL-guided MARL algorithm in this work. We also guarantee the satisfaction of hard safety requirements using control barrier functions (CBFs). Our proposed algorithm shows promising results in learning a better policy for each agent to reach its objective and ensure the safety of the system. Our contributions are summarized as follows:



Figure 1: *Traffic-jam* in CARLA simulator. Red vehicles stop on the street and blue vehicles should merge to the right lane with some other complex requirements apart from safety, such as eventually finishing the merging within a time horizon and the duration being blocked is less than a threshold, which can be naturally captured by temporal logic specifications.

- We design a multi-agent reinforcement learning algorithm that is guided by STL specifications, where the STL specifications include both safety requirements and the task that each agent aims to finish. We incorporate the STL-CBF safety shield to fulfill the safety specifications and provide safe actions for the agents.
- The proposed algorithm utilizes STL to check partial trajectories and provide robustness values as a corresponding reward during the training process.
- We present case studies on Multi-Agent Particle Environment (MPE) and CARLA testbeds. We demonstrate that compared with the baseline MARL algorithms and commonly used rewards, our proposed algorithm can learn better policies with larger rewards and safety rates.

2 Related Works

2.1 Multi-Agent Reinforcement Learning

There has been growing interest in the study of multi-agent reinforcement learning (MARL) since many real-world problems involve the interactions of multiple agents [1]. MARL approaches have been widely applied into various practical multi-agent systems, such as unmanned aerial vehicles [7, 8], complex traffic networks [9], autonomous driving [10], and so on. Despite these successful applications, one remained challenge in MARL is how to design good reward functions for complex tasks. Poorly-designed reward functions might lead to undesired behavior and be detrimental to safety-critical systems [11]. The complex interactions among agents and their diverse objectives make the reward shaping hard.

2.2 Temporal Logic for Reinforcement Learning

RL reward function usually relies on hand-engineered design or some traditional approaches like difference reward shaping [12]. In recent years, temporal logic specifications have been used extensively as training guidance in the context of single agent reinforcement learning for its power of expressiveness. In one direction, finite state automaton (FSA) is constructed to reward the agent (e.g., [13, 14, 15]). For example, authors of [14] convert the high-level linear temporal logic (LTL) specifications to the equivalent FSA, which is then used to guide the policy generation. This method enjoys the benefit of easy reward-generating automaton with high interpretability. In another direction,

the quantitative semantics of temporal logic formulas are captured to guide the policy training [5, 16]. For example, [5] considers the robustness value of the given signal temporal logic requirement as the reward to guide the training.

In the context of multi-agent reinforcement learning, very few works have been done to satisfy temporal logic specifications [6, 17]. For example, [6] proposes the first MARL algorithm for temporal logic specifications with correctness and convergence guarantees. However, [6] uses the LTL specifically designed to satisfy the non-Markovian, infinite-horizon specifications, which may not be the case in the real world applications. Also, it has not been empirically verified in MARL environments. In our work, we consider STL specifications and use their robustness values as the rewards instead. Compared with LTL, STL preserves quantitative semantics that can be used to establish a robust satisfaction value to quantify how well a trajectory fulfills a specification. This can further allow us to quantify the rewards more precisely and less sparser compared with LTL automaton-based rewards machine.

3 Preliminary and Problem Formulation

3.1 Multi-Agent Reinforcement Learning

Markov Games Partially observable Markov Games [18], a multi-agent extension of Markov Decision Process has been studied for multi-agent decision-making. A Markov game for N agents is defined by a set of states \mathcal{S} describing the possible configurations of all agents, a set of actions $\mathcal{A}_1, \dots, \mathcal{A}_N$ and a set of observations $\mathcal{O}_1, \dots, \mathcal{O}_N$ for each agent. Each agent i uses a stochastic policy $\pi_{\theta_i}: \mathcal{O}_i \times \mathcal{A}_i \mapsto [0, 1]$ parameterized by θ_i to choose actions, which produces the next state according to the state transition function $\mathcal{T}: \mathcal{S} \times \mathcal{A}_1 \times \dots \times \mathcal{A}_N \mapsto \mathcal{S}$. Each agent i obtains rewards as a function of the state and the agent's action, $r_i: \mathcal{S} \times \mathcal{A}_i \mapsto \mathbb{R}$, and receives a private observation correlated with the state, $o_i: \mathcal{S} \mapsto \mathcal{O}_i$. The initial states are determined by a distribution $\rho: \mathcal{S} \mapsto [0, 1]$. Each agent i aims to maximize its own total expected return, $R_i = \sum_{t=0}^T \gamma^t r_i^t$, where γ is a discount factor and T is the time horizon. Recent algorithms such as Multi-agent Deep Deterministic Policy Gradient (MADDPG) [19] and Multi-agent Proximal Policy Optimization (MAPPO) [20] have been designed to calculate neural network-based policies for MARL, and introductions to these algorithms are included in Appendix A.1.

3.2 Signal Temporal Logic

In this section, we introduce the syntax, semantics, and robustness metric of Signal Temporal Logic (STL), which is a powerful formal symbolism for specifying temporal logical requirements [21]. We first define the signal $\omega = s^0 s^1 \dots s^t$ as the state trajectory from starting state to time point t .

Definition 3.1. An STL formula is defined with the following syntax:

$$\varphi ::= \pi^\mu \mid \neg \pi^\mu \mid \varphi_1 \wedge \varphi_2 \mid \varphi_1 \vee \varphi_2 \mid \Diamond_{[a,b]} \varphi \mid \Box_{[a,b]} \varphi \mid \varphi_1 \mathcal{U}_{[a,b]} \varphi_2$$

Here, we denote an atomic predicate with π^μ , which can be represented as its underlying predicate function $\mu(\omega^t) \geq 0$, where ω^t is the value of signal ω at time t . The evaluation of all predicates occurs at each future step of the signal. We use \Box symbol to denote the *always* temporal operator, which indicates that a requirement must be met at all times in the future. Similarly, we use \Diamond to denote the *eventually* temporal operator, which requires that satisfaction must occur at some point in the future. Finally, we use \mathcal{U} to denote the *until* temporal operator, which specifies φ_1 is valid until φ_2 is true. Each temporal operator is associated with the bounded time interval $[a, b]$ with respect to the future. The satisfaction relation $(\omega, t) \models \varphi$ denotes if the signal ω satisfies φ at time t . In addition to the Boolean semantics, STL also owns the quantitative semantics (or *robust satisfaction values*) to evaluate the degree of the satisfaction [21, 22, 23]. It assigns real-valued measurements to the satisfaction (positive values) or violation (negative values) of the STL formula. In the evaluation section of this work, we utilize the robustness values to measure specification satisfactions. Readers can refer to the Appendix A.2 for the formal definition of quantitative semantics. A simple example of STL formula with its robustness computation is delayed into the Appendix A.3.

3.3 Problem Formulation of STL-guided MARL

STL-guided MARL: In this work, we define an STL-guided MARL for multi-agent decision-making problem such as the example shown in Fig. 1, to address the challenge of designing a reward function that utilize the strength of STL. In particular, we define a tuple $G =$

$(\mathcal{S}, \mathcal{A}, \mathcal{T}, \{r_i\}, \gamma, \{\varphi_i\}, \omega^{t-L+1:t})$ for an N -agent Markov game, where \mathcal{S} is the joint state space, \mathcal{A} is the joint action space, \mathcal{T} is the state transition function as the Markov game definition in the literature [18]. The key new components of the tuple definition include: $\omega^{t-L+1:t} = s^{t-L+1} \dots s^t$ is the partial state trajectory of length L , and φ_i is the STL formula for agent i . Take the *Traffic-jam* scenario as an example, the STL formula φ_i is the aggregation of several STL requirements, including reaching the destination, keeping safe distance to other agents, and waiting no more than T_{max} time steps after the broken-down vehicles. The details of the STL formula for different tasks will be introduced in Section 5. In the tuple G , reward $r_i = \rho(\varphi_i, \omega, t)$ represents the STL robustness value (the definition can be found in Appendix A.2), and each agent i aims to maximize its own total expected return $R_i = \sum_{t=0}^T \gamma^t r_i^t$ where γ is a discount factor and T is the time horizon.

4 Methodology

In this section, we first introduce the algorithm structure of STL-guided MARL algorithm. The major novelties of the algorithm are: (1) we leverage the quantitative semantics of STL specifications including both task specifications and safety specifications; (2) during the training process, the robustness values of partial trajectories of each agent are generated by checking the STL specifications and used as rewards; (3) we introduce the CBF safety shield that fulfills the safety specifications and provides safe actions for the agents. Our framework is shown in Fig 2.

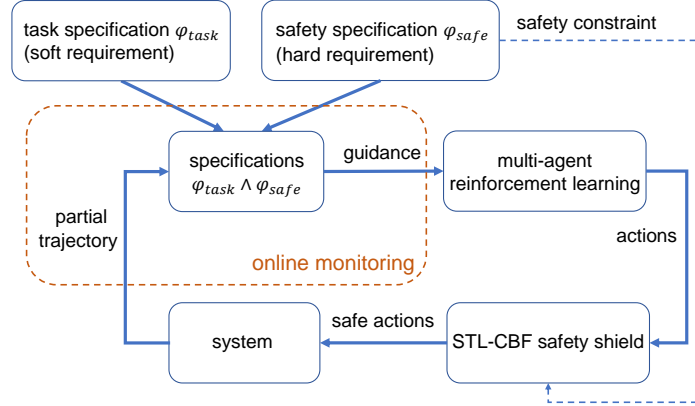


Figure 2: Methodology overview. The user-provided task specification and safety specification are expressed in STL formula φ_{task} and φ_{safe} , respectively. The robustness values of the (partial) trajectory/signal w.r.t. φ_{task} and φ_{safe} are used to generate reward and guide the MARL policy learning. The STL-CBF safety shield, which is constructed based on safety specification φ_{safe} , is involved to safeguard the decisions made by MARL.

4.1 STL-guided MARL

To address the challenge of defining a reward function for a multi-agent system that considers the objective of each individual agent and the complex interactions among agents, in this work, we check the partial trace based on the STL specifications, and provide the robustness value as the reward. It's notable that our method is generalizable to different MARL algorithms, e.g., MADDPG[19] and MAPPO[20].

At each time step of the training process, the trajectory contains the states of all the agents. Given the partial trajectory and STL specification φ_i , which might consist of both safety specification $\varphi_{i,safe}$ and task specification $\varphi_{i,task}$, the reward for agent i can be defined as

$$r_i^t = \rho(\varphi_i, \omega, t), \forall t \in [\tau, \tau + L - 1], \quad (1)$$

where ρ is the robustness value that is defined in Appendix A.2. Intuitively, given the partial trajectory, the more it satisfies the STL specifications, the larger reward it obtains. One reason we use partial trajectory robustness value rather full trajectory is that the former can provide *local* reward guidance, which is better to discriminate different states since *global* reward from full trajectory treats each state equally. From MARL algorithm design perspective, n-step methods allow for credit assignment over

¹To increase readability, we will omit truncation time indices $(t - L + 1 : t)$, i.e., we will use ω instead of $\omega^{t-L+1:t}$ to denote the partial trajectory with a slight notation abuse.

a longer time horizon such as in the A3C algorithm [24]. This enables the agent to better understand the consequences of its actions. Hence, in this work, we define the reward based on the robustness value given the partial trajectory ω . It should also be noted that the STL requirements encompass various types, including reaching the goal, safety requirements like maintaining a safe distance from other agents, and other temporal requirements. Detailed STL requirements for task specification and safety specification are illustrated by a case study in Subsection 4.3.

Algorithm 1: Pseudocode for STL-guided MARL

```

1 Orthogonal initialization for  $\theta_i$  and  $\phi_i$ , the parameters for policy  $\pi_i$  and critic  $V_i$ , respectively;
2 for  $episode = 1$  to  $M$  do
3   Episode initialization: replay buffer  $\mathcal{D} \leftarrow \emptyset$ ; initial state  $\mathbf{x}$ ; step  $t \leftarrow 1$ ; rollout step number  $L$ ;
4   while  $t \leq t_{\max}$  do
5      $t_{\text{start}} = t$ ;
6     Initialize an empty trajectory  $\omega$ ;
7     for  $t = t_{\text{start}}$  to  $t_{\text{start}} + L - 1$  do
8       For each agent  $i$ , select action  $a_{i_q}^t \leftarrow \pi_{\theta_i}(o_i^t)$  w.r.t the current policy and action
          exploration, send  $a_{i_q}^t$  into STL-CBF safety shield, and send back  $a_i^t$ ;
9       Execute actions  $\mathbf{a}^t = (a_1^t, \dots, a_N^t)$  chosen based on STL-CBF safety shield, append
           $\mathbf{x}^t$  to  $\omega$ , observe reward  $r_i^t = \rho(\varphi_i, \omega, t)$  for each agent  $i$  given agent  $i$ 's STL
          formula  $\varphi_i$ , observe new state  $\mathbf{x}^{t+1}$ ;
10       $\mathbf{x}^t \leftarrow \mathbf{x}^{t+1}$ ;  $t \leftarrow t + 1$ ;
11    end
12  end
13  Store  $\{(\mathbf{x}^\tau, \mathbf{a}^\tau, \mathbf{r}^\tau, \mathbf{x}^{\tau+1}) \mid \tau \in [t_{\text{start}}, \dots, t_{\text{start}} + L - 1]\}$  in  $\mathcal{D}$ ;
14  for agent  $i = 1$  to  $N$  do
15    Randomly sample mini-batch  $\{(\mathbf{x}^\tau, \mathbf{a}^\tau, \mathbf{r}^\tau, \mathbf{x}^{\tau+1}) \mid \tau \in [t, \dots, t + L - 1]\}$  from  $\mathcal{D}$ ;
16    Update critic by minimizing the objective  $\mathcal{L}^{\text{VF}}(\phi_i)$ ;
17    Update actor by maximizing the objective  $\mathcal{L}(\theta_i)$ ;
18  end
19 end

```

Discussion 1: Note that the online robustness value can be efficiently computed using existing approaches, see, e.g., [23], and there are some toolboxes that can be easily leveraged such as `pcheck`² and `stlcg`³.

In our work, we adopt the centralized training and decentralized execution paradigm. As depicted in Alg. 1, during the training phase, in rollout time steps t , each agent selects potentially unsafe action $a_{i_q}^t$ based on its local observations o_i^t . This action is then passed to the STL-CBF safety shield layer, and safe action a_i^t is returned and deployed such that the satisfaction of the STL safety specifications is guaranteed. The details of the STL-CBF safety shield layer will be presented in the next section. The global state $\mathbf{x}^t = (o_1^t, \dots, o_N^t)$, representing the aggregation of the local observations, is appended to the previous states to form the partial trajectory ω . By evaluating the partial trajectory against the STL requirements, each agent obtains its reward r_i^t .

The actor network is trained to maximize the following objective:

$$\mathcal{L}(\theta_i) = \frac{1}{B} \sum_{k=1}^B \min(r_{\theta_i, k} A_{i, k}, \text{clip}(r_{\theta, k}, 1 - \epsilon, 1 + \epsilon) A_{i, k}) + \sigma \frac{1}{B} \sum_{k=1}^B S[\pi_{\theta_i}(o_{i, k})], \quad (2)$$

where B is the batch size, $r_{\theta_i, k} = \frac{\pi_{\theta_i}(a_{i, k} | o_{i, k})}{\pi_{\theta_{i, \text{old}}}(a_{i, k} | o_{i, k})}$ denotes the ratio of the probability under the new and old policies respectively, $A_{i, k}$ is the advantage computed by GAE method [25], S is the policy

²<https://github.com/simonesilvetti/pcheck>

³<https://github.com/StanfordASL/stlcg>

entropy, and σ is the entropy coefficient hyperparameter. For the critic network, the loss function is:

$$\mathcal{L}^{\text{VF}}(\phi_i) = \frac{1}{B} \sum_{k=1}^B \max[(V_{\phi_i}(\mathbf{x}_{i,k}) - \hat{R}_{i,k})^2, (\text{clip}(V_{\phi_i}(\mathbf{x}_{i,k}), V_{\phi_{i_{\text{old}}}}(\mathbf{x}_{i,k}) - \epsilon, V_{\phi_{i_{\text{old}}}}(\mathbf{x}_{i,k}) + \epsilon) - \hat{R}_{i,k})^2], \quad (3)$$

where $\hat{R}_{i,k}$ is the discounted reward-to-go. For actor and critic network, we use the recurrent neural network (RNN) to take the input to enable the agents to effectively model and reason about sequential information in their interactions with the environment. By maintaining hidden states and updating them at each time step, RNN can capture the temporal dynamics and dependencies across multiple time steps.

4.2 STL-CBF Safety Shield

In multi-agent systems with complex dynamics, such as the *Traffic-jam* scenario depicted in Figure 1, ensuring system safety specification becomes paramount. One critical aspect of safety is maintaining a safe distance between agents. Consequently, we incorporate safety requirements into the Signal Temporal Logic (STL) formulas φ_{safe} , which will also be elaborated in Section 5. To satisfy these safety requirements specified in the STL formulas, such as “the distance between agents should always be greater than a threshold”, we first convert them to CBFs. Then, we employ the quadratic programming (CBF-QP) to ensure safety. By leveraging CBF-QP, we assess whether each discrete action guarantees system safety and filter out any unsafe actions accordingly.

Control barrier functions We model the low-level agent dynamic as a nonlinear control affine system: $\mathbf{x}^{t+1} = f(\mathbf{x}^t) + g(\mathbf{x}^t)\mathbf{u}^t$, where $\mathbf{x}^t \in \mathbb{R}^n$, $\mathbf{u}^t \in \mathcal{U}$ with $\mathcal{U} \subseteq \mathbb{R}^m$ denoting the set of permissible control inputs, f is the nominal unactuated dynamics, and g is the nominal actuated dynamics. Define the superlevel set $\mathcal{C}(t) \subset \mathbb{R}^n$ of a time-varying differentiable function $h(\mathbf{x}^t, t)$ by: $\mathcal{C}(t) = \{\mathbf{x}^t \in \mathbb{R}^n : h(\mathbf{x}^t, t) \geq 0\}$. A set $\mathcal{C} \subset \mathbb{R}^n$ is *forward invariant* if for every $\mathbf{x}^0 \in \mathcal{C}(0)$, the solution \mathbf{u}^t to the system satisfies $\mathbf{x}^t \in \mathcal{C}(t)$ for all $t \geq 0$. The system is *safe* with respect to the set $\mathcal{C}(t)$ if the set $\mathcal{C}(t)$ is forward invariant [26]. The function $h(\mathbf{x}^t, t)$ is a time-varying control barrier function (CBF) for the system on $\mathcal{C}(t)$ if there exists $\gamma \in [0, 1]$ [26, 27]:

$$\sup_{\mathbf{u}^t \in \mathcal{A}} [h(f(\mathbf{x}^t) + g(\mathbf{x}^t)\mathbf{u}^t, t+1) - h(\mathbf{x}^t, t)] \geq -\gamma h(\mathbf{x}^t, t). \quad (4)$$

Discussion 2: Note that the low-level control state space is different from the action space. We adopt the widely used kinematic bicycle model for its simplicity while still considering the non-holonomic vehicle behaviors [28] (see Appendix A.5). The state of the vehicle is $\mathbf{x}^t = [x^t, y^t, \psi^t, v^t]$, where x^t and y^t denote the coordinates of the vehicle’s center of gravity (c.g.) in an inertial frame (X, Y) , ψ^t and v^t represent the orientation and velocity of the vehicle. Here the vehicle’s state \mathbf{x}^t is part of its observation \mathbf{o}_i^t , whose definition is in Section 5.3. Also, the low-level control is different from Markov game action. The inputs \mathbf{u}^t of the low-level system are the acceleration a^t and the steering angle δ_j^t . Given each discrete action $a_{i,q}^t$ of Markov game, e.g., keep lane, change to left or right lane, acceleration or deceleration, there will be a corresponding continuous control input $\mathbf{u}_{i,q}^t$ using the trajectory planning method [29, 30].

Discussion 3: Safe reinforcement learning using CBFs has also drawn some attention recently, see, e.g., [31, 32]. However, these works consider single-agent setting and time-invariant CBFs, but we consider multi-agent setting and thus time-varying CBFs instead.

4.3 Case Study

We use a *Traffic-jam* scenario to explain the details of our methodology design and the definition of STL specifications that can generate reward values. As Fig. 1, in the *Traffic-jam* scenario, two broken-down vehicles block two lanes, a group of autonomous vehicles aim to cross the narrow road and arrive their destination as soon as possible, while maintaining the safety of the whole system. Agent i ’s observation at time t include (1) its own locations, velocities, accelerations, orientation $(\mathbf{p}_i^t, \mathbf{v}_i^t, \mathbf{a}_i^t, \psi_i^t)$ and its detection results using its onboard sensors (camera and Lidar); (2) other agent j ’s shared information $(\mathbf{p}_j^t, \mathbf{v}_j^t, \mathbf{a}_j^t, \psi_j^t), \forall j \in N$, (3) its destination $\mathbf{p}_{i_{\text{dest}}}$. Agent i ’s discrete action space include: $a_{i,1}$: keep speed and keep in current lane; $a_{i,2}$: change to left lane; $a_{i,3}$: change to right lane; $a_{i,4}$: brake; $a_{i,5} \sim a_{i,4+l}$: l different throttle values, representing l levels of acceleration and deceleration in the current lane.

We have the following requirements for each agent i : (1) (safety) distance between itself and the leading vehicle in its current lane and neighboring lanes should be always greater than a safe distance; (2) (task) eventually reach its destination; (3) (task) it should stop in front of the narrow road location \mathbf{p}_{road} ; (4) (task) its blocked duration t_{wait} in front of narrow road location \mathbf{p}_{road} should be less than T_{max} . These specifications can be easily converted to STL formulas accordingly:

$$\begin{aligned}
\text{(safety)} \quad \varphi_{i_1} &= \Box_{[0, T-1]} \|\mathbf{p}_i^t - \mathbf{p}_j^t\| - \frac{(v_j^t - v_i^t)^2}{a_{i_l}} \geq \epsilon_2, \forall j \in N, j \neq i \\
\text{(task)} \quad \begin{cases} \varphi_{i_2} &= \Diamond_{[0, T-1]} \|\mathbf{p}_i^t - \mathbf{p}_{dest}\| \leq \epsilon_1 \\ \varphi_{i_3} &= \Box_{[0, T-1]} (\neg(\|\mathbf{p}_i^t - \mathbf{p}_{road}\| \leq L) \vee (\Diamond_{[0, \tau]} v_i^t \leq 0)) \\ \varphi_{i_4} &= \Box_{[0, T-1]} (\neg(\|\mathbf{p}_i^t - \mathbf{p}_{road}\| \leq L) \vee (t_{wait} < T_{max})) \end{cases} \quad (5)
\end{aligned}$$

CBF for safety Here we show how to define the barrier functions to fulfill the safety requirements in STL specifications. As shown in Fig 3, during the lane keeping mode, the ego vehicle should keep a safe distance to the vehicle in the front in its current lane; while it's changing the lane, it should keep a safe distance to both the vehicles in its front and back. We use fv and bv to denote the front and back vehicles in the target lane respectively. The safe distance to the front vehicle can be expressed as $D_{fv} = (1 + \epsilon)v^t + \frac{(v^t - v_{fv}^t)^2}{2a_l}$, and the safe distance to the back vehicle is $D_{bv} = (1 + \epsilon)v^t + \frac{(v_{bv}^t - v^t)^2}{2a_l}$. Note that a_l and v^t are the ego vehicle's acceleration limit and current speed respectively, and v_{fv}^t, v_{bv}^t denote the velocity of vehicle in the front and back respectively. Finally, the CBFs can be expressed as: $h_{fv}(\mathbf{x}^t, t) = (x_{fv}^t - x^t)^2 - D_{fv}^2(v^t, v_{fv}^t)$ and $h_{bv}(\mathbf{x}^t, t) = (x^t - x_{bv}^t)^2 - D_{bv}^2(v^t, v_{bv}^t)$.

For each discrete action $a_{i_q}^t$, after being mapped to the corresponding continuous control input $\mathbf{u}_{i_q}^t$ [29, 30], then the following CBF-QP is solved to return a safe control input:

$$\begin{aligned}
\min \quad & \|\mathbf{u}^t - \mathbf{u}_{i_q}^t\|_2^2 \\
\text{s.t.} \quad & \sup_{\mathbf{u}^t \in \mathcal{U}} [h(f(\mathbf{x}^t) + g(\mathbf{x}^t)\mathbf{u}^t, t+1) - h(\mathbf{x}^t, t)] \geq -\gamma h(\mathbf{x}^t, t). \quad (6)
\end{aligned}$$

Then, we can have the safety guarantees [26, 27] and its proof is presented in Appendix A.4:

Proposition 1. Assume $h(\mathbf{x}^t, t)$ is a valid time-varying CBF on \mathcal{C} . Then any controller $\mathbf{u}^t(\mathbf{x}^t)$ from (6) for all $\mathbf{x}^t \in \mathcal{C}$ will render the set \mathcal{C} forward invariant, i.e., the system is safe.

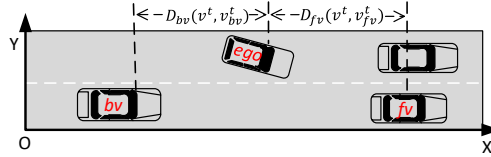


Figure 3: Lane change in *Traffic-jam* scenario.

5 Experiments and Case Studies

5.1 Testbeds and Common Experiment Setup

Testbed environment: we evaluate the performance of STL-guided MARL algorithm on two benchmarks: the multi-agent particle-world environment (MPE) [19] and CARLA [33]. For MPE, we develop two new scenarios, namely “Simple Coordination II” and “Simple Spread II”, which feature an increased number of stages for the agents to reach. These new scenarios introduce additional temporal requirements compared to the existing tasks. Within CARLA, we consider the *Traffic-jam* scenario, which is characterized by intricate interactions, demanding stringent safety requirements, and imposing higher temporal constraints on the agents’ decision-making processes.

Common experimental setup: we conduct a comparative analysis of the STL-guided MARL algorithm and the MARL algorithm with the original task reward in both testbeds. In STL-guided MARL, the STL reward are the weighted sum of the robustness values of all the STL specifications. We denote the STL reward as $r_i^t = \sum_j c_j \rho(\varphi_{i_j}, \omega, t) + b$, where c_j are weights and b is a constant. To ensure a fair comparison, the original reward function are based on widely adopted designs found in

the existing literature. We evaluate the performance of both methods by examining the episode return. It's worth noting that, for consistency, we compute the return using the STL reward in both algorithms. This approach allows us to quantify the extent to which the agents learn to fulfill the designer's goals. Essentially, a larger return signifies a greater level of fulfillment of the STL requirements. For our experiments, we utilize a server equipped with Intel Core i9-10900X processors and four NVIDIA RTX2080Ti GPUs. The experiments are conducted using Python 3.6.0, PyTorch 1.6.0, and CUDA 11.0. In the following sections for the two testbeds, we first introduce the reward function used for baseline MARL algorithms, then introduce the STL specifications of our proposed Alg.1, finally we present our experiment results. The parameters for experiment are in appendix A.6.

5.2 MPE Testbed

Environment: In MPE, we design two new tasks, simple coordination II and simple spread II to evaluate our algorithm. In both tasks, the observation of agent i include the relative positions to other agents and the landmarks, the discrete actions space are: stay, left, right, up and down.

Baselines: In both tasks, N agents need to first cover N landmarks in the first stage, and then another N landmarks in the second stage with least collisions. The difference is: in simple coordination II, agent and landmark are paired so agent only targets at its own corresponding landmark; for simple spread II, agents learn to infer the landmark they must cover, and move there while avoiding other agents. The reward function for simple coordination II is: $r = -c_1 \sum_{i=1}^N (|\mathbf{p}_i - \mathbf{p}_{i,\text{landmark, goal}}|) + c_2 \sum_{i=1}^N (|\mathbf{p}_i - \mathbf{p}_{i,\text{landmark, others}}|)$ where \mathbf{p}_i is location of agent i , $\mathbf{p}_{i,\text{landmark, goal}}$ is location of the current goal landmark of agent i , $\mathbf{p}_{i,\text{landmark, goal}}$ is location of the other landmark. The reward function for simple spread II is $r = -c_1 \sum_{i=1}^N (\min_{j \in N} |\mathbf{p}_j - \mathbf{p}_{i,\text{landmark, goal}}|) + c_2 \sum_{i=1}^N (\min_{j \in N} |\mathbf{p}_j - \mathbf{p}_{i,\text{landmark, others}}|)$ where \mathbf{p}_j is location of agent j , $\mathbf{p}_{i,\text{landmark, goal}}$ is location of the landmark i in current goal stage, $\mathbf{p}_{i,\text{landmark, others}}$ is location of the other stage's landmark i . In both tasks, for a collision, there will be a -1 penalty added on the current reward. The reward function is based on the reward designed in the existing works[19, 16]. We use MADDPG[19] as our baseline algorithm.

STL-guided MARL: For both tasks, given a whole trajectory of length T of agent i , the requirements include: (1) All first part of N landmarks are eventually visited by their corresponding agent; (2) All second part of N landmarks are eventually covered by their corresponding agent; (3) no collision between agents nearby (the distance is always greater than the safety threshold); (4) The first three landmarks should be visited at least once before the second three landmarks are visited.

Therefore, we write the specifications for simple coordination as:

$$\varphi_{i_1} = \Diamond_{[0,T]} \bigwedge_{1,2,\dots} |\mathbf{p}_i^t - \mathbf{p}_{i,\text{landmark, first}}| \leq \epsilon_1, \quad \varphi_{i_2} = \Box_{[T-5,T]} \bigwedge_{1,2,\dots} |\mathbf{p}_i^t - \mathbf{p}_{i,\text{landmark, second}}| \leq \epsilon_2. \quad (7)$$

Similarly, the STL specifications for simple spread II are:

$$\begin{aligned} \varphi_{i_1} &= \Diamond_{[0,T]} \bigwedge_{1,2,\dots} \min_{j \in N} |\mathbf{p}_j^t - \mathbf{p}_{i,\text{landmark, first}}| \leq \epsilon_1, \\ \varphi_{i_2} &= \Diamond \Box_{[T-5,T]} \bigwedge_{1,2,\dots} \min_{j \in N} |\mathbf{p}_j^t - \mathbf{p}_{i,\text{landmark, second}}| \leq \epsilon_2. \end{aligned} \quad (8)$$

The common safety requirement is: $\varphi_{i_3} = \Box_{[0,T]} \bigwedge_{1,2,\dots} |\mathbf{p}_i^t - \mathbf{p}_j^t| \geq D_{\text{saf}}, \forall j \in N$.

Experiment Results: We train the algorithms for 30000 episodes, with episode length of 25 to evaluate their performance. Fig 4 provides insights into the mean and variance of the average returns for the two tasks. Notably, the STL-guided MARL algorithm demonstrates superior performance compared to baseline algorithm in terms of episode return. Specifically, the agents trained with the STL-guided MARL approach exhibit a remarkable ability to cover the second stage landmarks after visiting the first stage. On the other hand, the agents trained with baseline algorithm MADDPG struggle to cover the second stage landmarks and tend to hover around the first stage.

This disparity in performance highlights the advantage of the STL-guided approach in facilitating the policy learning. By incorporating STL specifications, the agents are encouraged to adhere to specific behavioral patterns that result in more successful navigation and completion of the tasks. In contrast, the agents trained with a comparison reward, without the STL-guided framework, lack the guidance necessary to achieve optimal performance and struggle to exhibit the desired behavior.

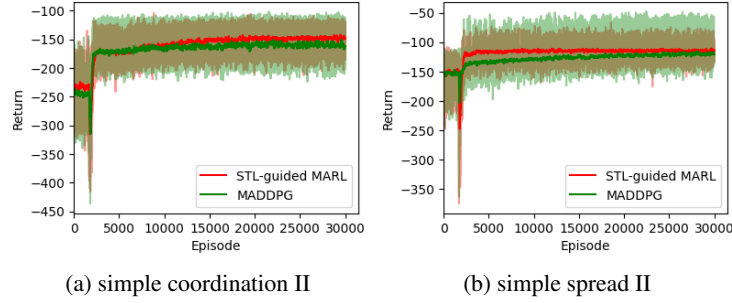


Figure 4: Training results in MPE.

Table 1: Mean episode return in MPE. STL-guided MARL shows higher mean episode return in both tasks compared with baseline algorithm, demonstrating the advantages of our method in helping agent learn a better policy to fulfill the designer’s intentions.

Methods	Simple coordination II	Simple spread II
STL-guided MARL	-162.01 ± 29.93	-120.47 ± 18.13
MADDPG	-169.17 ± 33.64	-128.36 ± 17.90

5.3 CARLA Testbed

The *Traffic-jam* scenario settings and STL specifications are illustrated in Section 4.3.

Baselines: We adopt the reward that are widely used in the existing literature for lane merging case[34, 35]. The reward for agent i are defined as follow: $r_i = w_1 r_i^{\text{speed}} + w_2 r_i^{\text{collision}} + w_3 r_i^{\text{dest}}$, where $w_1, w_2, w_3 \in \mathbb{R}$ are the weights, $r_i^{\text{speed}} = \frac{|v_i|}{v_{max}}$, $r_i^{\text{collision}} = -I_{col}$ with I_{col} being the collision intensity collected by collision sensor, $r_i^{\text{dest}} = -|p_i - p_{dest}| + c$ with c being a constant. we use MAPPO algorithm [20], MAA2C algorithm[36], and MAPPO algorithm without STL-CBF safety shield as our baseline algorithms.

Experiment Results: All the algorithms are trained 100 episodes with the episode length of 150 steps. The training results are shown in Table 2. It can be observed that: (1) In *Traffic-jam* scenario, MARL algorithms with STL-CBF safety shield largely outperforms the algorithm without it in both mean episode return and safety rate, therefore demonstrate the effectiveness of our proposed STL-CBF safety shield in ensuring the safety of the system. Note that the reason that causes 3% safety loss might be the models mismatch, i.e., our identified system model is not exactly the same with the real model run in the simulator, which is hard to obtain. (2) The STL-guided MARL algorithm consistently outperforms the baseline algorithms in mean episode return. The superior performance of the STL-guided MARL algorithm can be attributed to its expressiveness and ability to capture the designer’s goal. By leveraging STL as a guidance framework, the algorithm is able to incorporate high-level specifications and constraints into the learning process. This enables the agent to learn a policy that aligns more closely with the desired behavior outlined by the designer. Thus, the STL-guided MARL algorithm demonstrates its effectiveness in improving the learning process and enabling the agent to achieve better performance.

Table 2: Mean episode return and safety rate in *Traffic-jam* scenario.

Methods	Mean episode return			Safety rate
	Agent 1	Agent 2	Agent 3	
STL-guided MARL	1469.98 ± 43.87	3577.53 ± 580.04	3699.26 ± 588.62	97%
MAPPO	1244.12 ± 174.18	1838.96 ± 392.22	2245.07 ± 150.75	74%
MAA2C	1131.51 ± 389.62	1645.80 ± 693.49	2713.19 ± 465.45	88%
MAPPO w/o CBF	853.30 ± 421.46	1241.91 ± 223.38	2102.25 ± 713.09	65%

6 Conclusion

We propose a safe multi-agent reinforcement learning algorithm that leverages signal temporal logic (STL) specifications to guide the learning process and ensure the satisfaction of safety requirements and task objectives for each agent. By incorporating STL-CBF safety shields, our algorithm provides additional safety guarantees in the system. Through case studies, we demonstrate that our approach outperforms traditional MARL methods with hand-engineered rewards, as it learns better policies with higher average rewards and ensures the system safety. Our work highlights the potential of

using temporal logic and formal languages in MARL to address the challenges of reward design and safety in complex multi-agent systems. **Limitations:** The algorithm assumes a centralized training distributed execution setting, in the future we will explore more about decentralized or distributed training frameworks. **Broader impacts:** To the best of the authors’ knowledge, there is no potential negative societal impact in this work.

References

- [1] Kaiqing Zhang, Zhuoran Yang, and Tamer Başar. Multi-agent reinforcement learning: A selective overview of theories and algorithms. *Handbook of reinforcement learning and control*, pages 321–384, 2021.
- [2] David Silver, Satinder Singh, Doina Precup, and Richard S Sutton. Reward is enough. *Artificial Intelligence*, 299:103535, 2021.
- [3] Songtao Lu, Kaiqing Zhang, Tianyi Chen, Tamer Başar, and Lior Horesh. Decentralized policy gradient descent ascent for safe multi-agent reinforcement learning. In *Proceedings of the AAAI Conference on Artificial Intelligence*, volume 35, pages 8767–8775, 2021.
- [4] Zhili Zhang, Songyang Han, Jiangwei Wang, and Fei Miao. Spatial-temporal-aware safe multi-agent reinforcement learning of connected autonomous vehicles in challenging scenarios. *arXiv preprint arXiv:2210.02300*, 2022.
- [5] Anand Balakrishnan and Jyotirmoy V Deshmukh. Structured reward shaping using signal temporal logic specifications. In *2019 IEEE/RSJ International Conference on Intelligent Robots and Systems (IROS)*, pages 3481–3486. IEEE, 2019.
- [6] Lewis Hammond, Alessandro Abate, Julian Gutierrez, and Michael Wooldridge. Multi-agent reinforcement learning with temporal logic specifications. *arXiv preprint arXiv:2102.00582*, 2021.
- [7] Jingjing Cui, Yuanwei Liu, and Arumugam Nallanathan. Multi-agent reinforcement learning-based resource allocation for uav networks. *IEEE Transactions on Wireless Communications*, 19(2):729–743, 2019.
- [8] Han Qie, Dianxi Shi, Tianlong Shen, Xinhai Xu, Yuan Li, and Liuqing Wang. Joint optimization of multi-uav target assignment and path planning based on multi-agent reinforcement learning. *IEEE access*, 7:146264–146272, 2019.
- [9] Tianshu Chu, Jie Wang, Lara Codecà, and Zhaojian Li. Multi-agent deep reinforcement learning for large-scale traffic signal control. *IEEE Transactions on Intelligent Transportation Systems*, 21(3):1086–1095, 2019.
- [10] Shai Shalev-Shwartz, Shaked Shammah, and Amnon Shashua. Safe, multi-agent, reinforcement learning for autonomous driving. *arXiv preprint arXiv:1610.03295*, 2016.
- [11] Dario Amodei, Chris Olah, Jacob Steinhardt, Paul Christiano, John Schulman, and Dan Mané. Concrete problems in ai safety. *arXiv preprint arXiv:1606.06565*, 2016.
- [12] Scott Proper and Kagan Tumer. Modeling difference rewards for multiagent learning. In *AAMAS*, pages 1397–1398, 2012.
- [13] Rodrigo Toro Icarte, Torny Klassen, Richard Valenzano, and Sheila McIlraith. Using reward machines for high-level task specification and decomposition in reinforcement learning. In *International Conference on Machine Learning*, pages 2107–2116. PMLR, 2018.
- [14] Xiao Li, Zachary Serlin, Guang Yang, and Calin Belta. A formal methods approach to interpretable reinforcement learning for robotic planning. *Science Robotics*, 4(37):eaay6276, 2019.
- [15] Mingyu Cai, Shaoping Xiao, Junchao Li, and Zhen Kan. Safe reinforcement learning under temporal logic with reward design and quantum action selection. *Scientific reports*, 13(1):1925, 2023.
- [16] Xiao Li, Cristian-Ioan Vasile, and Calin Belta. Reinforcement learning with temporal logic rewards. In *2017 IEEE/RSJ International Conference on Intelligent Robots and Systems (IROS)*, pages 3834–3839. IEEE, 2017.

- [17] Ingy ElSayed-Aly, Suda Bharadwaj, Christopher Amato, Rüdiger Ehlers, Ufuk Topcu, and Lu Feng. Safe multi-agent reinforcement learning via shielding. *arXiv preprint arXiv:2101.11196*, 2021.
- [18] Michael L Littman. Markov games as a framework for multi-agent reinforcement learning. In *Machine learning proceedings 1994*, pages 157–163. Elsevier, 1994.
- [19] Ryan Lowe, Yi I Wu, Aviv Tamar, Jean Harb, OpenAI Pieter Abbeel, and Igor Mordatch. Multi-agent actor-critic for mixed cooperative-competitive environments. *Advances in neural information processing systems*, 30, 2017.
- [20] Chao Yu, Akash Velu, Eugene Vinitsky, Jiaxuan Gao, Yu Wang, Alexandre Bayen, and Yi Wu. The surprising effectiveness of ppo in cooperative multi-agent games. *Advances in Neural Information Processing Systems*, 35:24611–24624, 2022.
- [21] Oded Maler and Dejan Nickovic. Monitoring temporal properties of continuous signals. In *Formal Techniques, Modelling and Analysis of Timed and Fault-Tolerant Systems*, pages 152–166. Springer, 2004.
- [22] Georgios E Fainekos and George J Pappas. Robustness of temporal logic specifications for continuous-time signals. *Theoretical Computer Science*, 410(42):4262–4291, 2009.
- [23] Jyotirmoy V Deshmukh, Alexandre Donzé, Shromona Ghosh, Xiaoqing Jin, Garvit Juniwal, and Sanjit A Seshia. Robust online monitoring of signal temporal logic. *Formal Methods in System Design*, 51(1):5–30, 2017.
- [24] Volodymyr Mnih, Adria Puigdomenech Badia, Mehdi Mirza, Alex Graves, Timothy Lillicrap, Tim Harley, David Silver, and Koray Kavukcuoglu. Asynchronous methods for deep reinforcement learning. In *International conference on machine learning*, pages 1928–1937. PMLR, 2016.
- [25] John Schulman, Philipp Moritz, Sergey Levine, Michael Jordan, and Pieter Abbeel. High-dimensional continuous control using generalized advantage estimation. *arXiv preprint arXiv:1506.02438*, 2015.
- [26] Aaron D Ames, Xiangru Xu, Jessy W Grizzle, and Paulo Tabuada. Control barrier function based quadratic programs for safety critical systems. *IEEE Transactions on Automatic Control*, 62(8):3861–3876, 2016.
- [27] Jun Zeng, Bike Zhang, and Koushil Sreenath. Safety-critical model predictive control with discrete-time control barrier function. In *2021 American Control Conference (ACC)*, pages 3882–3889. IEEE, 2021.
- [28] J Kong, M Pfeiffer, G Schildbach, and F Borrelli. Autonomous driving using model predictive control and a kinematic bicycle vehicle model. In *Intelligent Vehicles Symposium, Seoul, Korea*, 2015.
- [29] Shilp Dixit, Saber Fallah, Umberto Montanaro, Mehrdad Dianati, Alan Stevens, Francis Mccullough, and Alexandros Mouzakitis. Trajectory planning and tracking for autonomous overtaking: State-of-the-art and future prospects. *Annual Reviews in Control*, 45:76–86, 2018.
- [30] Gianluca Cesari, Georg Schildbach, Ashwin Carvalho, and Francesco Borrelli. Scenario model predictive control for lane change assistance and autonomous driving on highways. *IEEE Intelligent transportation systems magazine*, 9(3):23–35, 2017.
- [31] Richard Cheng, Gábor Orosz, Richard M Murray, and Joel W Burdick. End-to-end safe reinforcement learning through barrier functions for safety-critical continuous control tasks. In *Proceedings of the AAAI conference on artificial intelligence*, volume 33, pages 3387–3395, 2019.
- [32] Yousef Emam, Gennaro Notomista, Paul Glotfelter, Zsolt Kira, and Magnus Egerstedt. Safe reinforcement learning using robust control barrier functions. *IEEE Robotics and Automation Letters*, 99:1–8, 2022.
- [33] Alexey Dosovitskiy, German Ros, Felipe Codevilla, Antonio Lopez, and Vladlen Koltun. Carla: An open urban driving simulator. In *Conference on robot learning*, pages 1–16. PMLR, 2017.
- [34] Sai Krishna Sumanth Nakka, Behdad Chalaki, and Andreas A Malikopoulos. A multi-agent deep reinforcement learning coordination framework for connected and automated vehicles at merging roadways. In *2022 American Control Conference (ACC)*, pages 3297–3302. IEEE, 2022.

- [35] Dong Chen, Mohammad Hajidavalloo, Zhaojian Li, Kaian Chen, Yongqiang Wang, Longsheng Jiang, and Yue Wang. Deep multi-agent reinforcement learning for highway on-ramp merging in mixed traffic. *arXiv preprint arXiv:2105.05701*, 2021.
- [36] Georgios Papoudakis, Filippos Christianos, Lukas Schäfer, and Stefano V Albrecht. Benchmarking multi-agent deep reinforcement learning algorithms in cooperative tasks. *arXiv preprint arXiv:2006.07869*, 2020.
- [37] John Schulman, Filip Wolski, Prafulla Dhariwal, Alec Radford, and Oleg Klimov. Proximal policy optimization algorithms. *arXiv preprint arXiv:1707.06347*, 2017.
- [38] Alexandre Donzé and Oded Maler. Robust satisfaction of temporal logic over real-valued signals. In *Formal Modeling and Analysis of Timed Systems: 8th International Conference, FORMATS 2010, Klosterneuburg, Austria, September 8-10, 2010. Proceedings* 8, pages 92–106. Springer, 2010.

A Appendix

A.1 Preliminary of MARL Algorithms

Multi-agent Proximal Policy Optimization MAPPO is an extension of Proximal Policy Optimization (PPO) in multi-agent settings [20]. It resembles the core structure of PPO with a local policy $\pi^{\theta_i}(s_i)$ for each agent i , while it leverages the merit of multi-agent environment by having the centralized value function $V_i^{\phi_i}(s)$ that takes in the global state s during training. Consider a game with N agents. Let $\{\pi^{\theta_i} | i \in [1, \dots, N]\}$ be the set of all agents' policies parameterized by $\theta = \{\theta_i | i \in [1, \dots, N]\}$, and let $\{V^{\phi_i} | i \in [1, \dots, N]\}$ be the set of centralized value functions parameterized by $\phi = \{\phi_i | i \in [1, \dots, N]\}$. The ‘‘Clipped Surrogate Objective’’ [37] $L^{\text{CLIP}}(\theta_i)$ uniquely adopted to train the actor network in MAPPO is defined as:

$$\mathcal{L}(\theta_i) = \mathbb{E}_{\mathbf{x}, a \sim \mathcal{D}} [\min(r_i(\theta_i) \hat{A}_i, \text{clip}(r_i(\theta_i), 1 - \varepsilon, 1 + \varepsilon) \hat{A}_i) + \sigma S[\pi^{\theta_i}(\mathbf{x})]), \quad (9)$$

where $r_i(\theta_i) = \frac{\pi^{\theta_i}(\mathbf{x})}{\pi^{\theta_i^{\text{old}}}(\mathbf{x})}$ denotes the probability ratio between agent i 's current and previous policy, $\hat{A}_i = [(r + V^{\phi_i}(\mathbf{x}')) - V^{\phi_i}(\mathbf{x})]$ is the estimated advantage function for agent i , and $S[\pi^{\theta_i}(\mathbf{x})]$ is the entropy penalty. The objective of value function \mathcal{L}^{VF} is defined as the squared error:

$$\mathcal{L}^{\text{VF}}(\phi_i) = \mathbb{E}_{\mathbf{x}, r, \mathbf{x}' \sim \mathcal{D}} (V^{\phi_i}(\mathbf{x}) - (r + V^{\phi_i}(\mathbf{x}')))^2. \quad (10)$$

Multi-agent Deep Deterministic Policy Gradient The core idea of MADDPG is learning a centralized Q function for each agent which conditions on global information to alleviate the non-stationary problem and stabilize training. Consider a game with N agents with policies parameterized by $\theta = \{\theta_1, \dots, \theta_N\}$, and let $\pi = \{\pi_1, \dots, \pi_N\}$ be the set of all agents' policies. Then the gradient of the expected return for agent i with policy π_i , $J(\theta_i) = E[R_i]$ as:

$$\nabla_{\theta_i} J(\theta_i) = \mathbb{E}_{\mathbf{x}, a \sim \mathcal{D}} (\nabla_{\theta_i} \mu_i(o_i) \nabla_{a_i} Q_i^{\mu}(\mathbf{x}, a_1, \dots, a_N) |_{a_i = \mu_i(o_i)}); \quad (11)$$

here $Q_i^{\mu}(\mathbf{x}, a_1, \dots, a_N)$ is a centralized action-value function that takes the actions of all agents and the global state information \mathbf{x} (i.e., $\mathbf{x} = (o_1, \dots, o_N)$) as inputs, and outputs the Q value for agent i . The experience replay buffer \mathcal{D} contains the tuples $(\mathbf{x}, \mathbf{x}', a_1, \dots, a_N, r_1, \dots, r_N)$, recording experiences of all agents. The centralized action-value function Q_i^{μ} is updated as:

$$\begin{aligned} \mathcal{L}(\theta_i) &= \mathbb{E}_{\mathbf{x}, a, r, \mathbf{x}'} [(Q_i^{\mu}(\mathbf{x}, a_1, \dots, a_N) - y)^2], \\ y &= r_i + \gamma Q_i^{\mu'}(\mathbf{x}', a'_1, \dots, a'_N) |_{a'_i = \mu'_i(o_i)}; \end{aligned} \quad (12)$$

where $\mu' = \{\mu_{\theta'_1}, \dots, \mu_{\theta'_N}\}$ is the set of target policies with delayed parameters θ'_i .

A.2 STL quantitative semantics

The STL quantitative semantics (i.e. STL robustness) [38] is formally defined as follows.

$$\begin{aligned} \rho(x \sim c, \varphi, t) &= \pi(\omega[t]) - c \\ \rho(\neg\varphi, \omega, t) &= -\rho(\varphi, \omega, t) \\ \rho(\varphi_1 \wedge \varphi_2, \omega, t) &= \min\{\rho(\varphi_1, \omega, t), \rho(\varphi_2, \omega, t)\} \\ \rho(\varphi_1 \vee \varphi_2, \omega, t) &= \max\{\rho(\varphi_1, \omega, t), \rho(\varphi_2, \omega, t)\} \\ \rho(\Box_I \varphi, \omega, t) &= \min_{t' \in (t, t+I)} \rho(\varphi, \omega, t') \\ \rho(\Diamond_I \varphi, \omega, t) &= \max_{t' \in (t, t+I)} \rho(\varphi, \omega, t') \\ \rho(\varphi_1 \mathcal{U}_I \varphi_2, \omega, t) &= \sup_{t' \in (t+I) \cap \mathbb{T}} (\min\{\rho(\varphi_2, \omega, t'), \inf_{t'' \in [t, t']} (\rho(\varphi_1, \omega, t''))\}) \end{aligned}$$

Here, ρ denotes the robustness value, which is evaluated *recursively*. φ , φ_1 , and φ_2 denote different STL formulas. Additionally, x is a signal variable that is compared against the constant threshold c .

A.3 A simple STL example

To demonstrate how STL formulas can be used to specify safety properties in multi-agent scenarios, we provide an illustrative example, as shown in Fig. 5. The left figure shows the trajectories of two vehicles, and the right figure presents the distance between them. In this scenario, we define the STL formula $\Box_{[0,25]}(|p_1 - p_2| < D_{safe})$ to specify the safe distance requirement. Here, D_{safe} denotes the safe distance between two vehicles and is set to be 3.5 in this example. Additionally, we use p_1 and p_2 to denote the positions of two vehicles. This formula specifies that *the distance between two vehicles must always remain greater than 3.5 to ensure safety*. This requirement is considered as a *hard* requirement and can be effectively enforced at all times throughout the specified interval by our proposed algorithm.

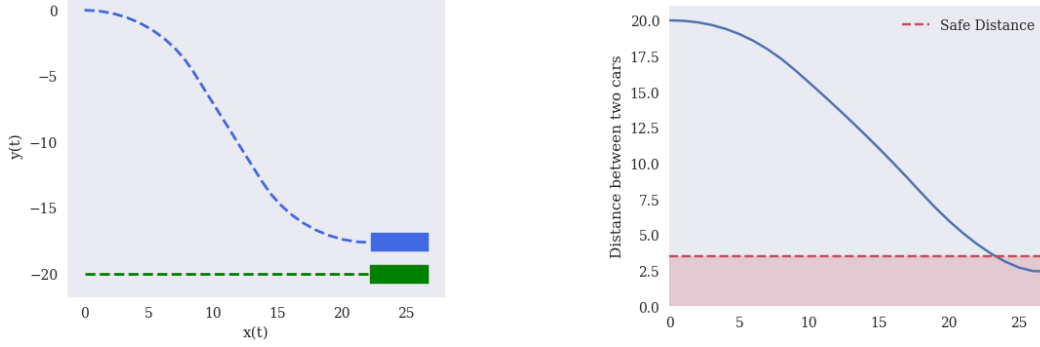


Figure 5: An example of two cars getting closer to each other (left figure), thus violating the hard requirement on safe distance (right figure). The blue and green blocks represent vehicle 1 and vehicle 2, respectively. The red region represents the violation of safe distance requirement.

A.4 CBF safety proof

Proposition 1. Assume $h(\mathbf{x}^t, t)$ is a valid time-varying CBF on \mathcal{C} . Then any controller $\mathbf{u}^t(\mathbf{x}^t)$ from (6) for all $\mathbf{x}^t \in \mathcal{C}$ will render the set \mathcal{C} forward invariant, i.e., the system is safe.

Proof. For any control policy $\mathbf{u}(\mathbf{x}^t)$ from (6), it satisfies that

$$h(f(\mathbf{x}^t) + g(\mathbf{x}^t)\mathbf{u}(\mathbf{x}^t), t+1) - h(\mathbf{x}^t, t) \geq -\gamma h(\mathbf{x}^t, t), \quad (13)$$

where $\gamma \in [0, 1]$. The above condition is equivalent to $h(\mathbf{x}^{t+1}, t+1) - h(\mathbf{x}^t, t) \geq -\gamma h(\mathbf{x}^t, t)$. Since we have that $\mathbf{x}^t \in \mathcal{C}(t)$ for $t = 0$, i.e., the initial state is safe or $h(\mathbf{x}^0, 0) \geq 0$, we thereafter can recursively derive that:

$$h(\mathbf{x}^t, t) \geq (1 - \gamma)h(\mathbf{x}^{t-1}, t-1) \geq (1 - \gamma)^2 h(\mathbf{x}^{t-2}, t-2) \geq \dots \geq (1 - \gamma)^t h(\mathbf{x}^0, 0) \geq 0, \quad (14)$$

which means that the safety can be preserved for any t . This ends the proof. \square

A.5 Bicycle model

We adopt the bicycle model in this work to describe the dynamics of the vehicles in CARLA, the discrete-time bicycle model equations with steering angle δ and acceleration a as control inputs are given by:

$$\begin{aligned} x^{t+1} &= x^t + T \cdot v^t \cdot \cos(\psi^t) \\ y^{t+1} &= y^t + T \cdot v^t \cdot \sin(\psi^t) \\ \psi^{t+1} &= \theta^t + T \cdot \frac{v^t}{l} \cdot \tan(\delta^t) \\ v^{t+1} &= v^t + T \cdot a^t \end{aligned}$$

In these equations:

- t represents the discrete time step index.
- x^t and y^t are the coordinates of the bicycle’s position at time step t .
- ψ^t is the heading angle (yaw angle) of the bicycle at time step t .
- v^t is the velocity of the bicycle at time step t .
- δ^t is the steering angle (steering input) at time step t .
- a^t is the acceleration (acceleration input) at time step t .
- T is the time step duration between consecutive updates of the model.
- l is the length of the wheelbase, which is the distance between the front and rear axles.

A.6 Implementation details

In MPE testbed, simple spread II and simple coordination II tasks’ original rewards for baseline algorithms contains weighted sum of the distance to first stage’s landmarks and second stage’s landmarks, and the collision penalty, as illustrated in Section 5.2. The two weighted term is: $c_1 = 1$ and $c_2 = 0.2$, we try different weight term ratios and we use the one with the best performance as the baseline to compare with our proposed STL reward. Hence, the other weighted parameters only have lower mean episode rewards. For the STL reward $r_i^t = \sum_j c_j \rho(\varphi_{i,j}, \omega_j, t) + b$, we set the weight for STL specifications and the constant as: $c_1 = 1, c_2 = 1, c_3 = 1, b = 0$. It’s worth noting that, in order to verify the generalizability of the STL-guided approach under different multi-agent reinforcement learning algorithm frameworks, we adopt the loss function same as in MADDPG (see Eq. 11 and Eq. 12) in our STL-guided MARL for MPE testbed. The hyperparameters for STL-guided MARL and baseline MADDPG are summarized in Table 3. We use Fig. 6 to further illustrate the effectiveness of the STL-guided MARL algorithm.

Table 3: Common hyperparameters for STL-guided MARL, MADDPG in MPE testbed

Hyperparameter	Value
actor learning rate	1e-3
critic learning	1e-3
critic loss	mse loss
discount Factor	0.95
batch size	1024
buffer capacity	1e6
optimizer	Adam
fc layer dim	64
activation layer	ReLU

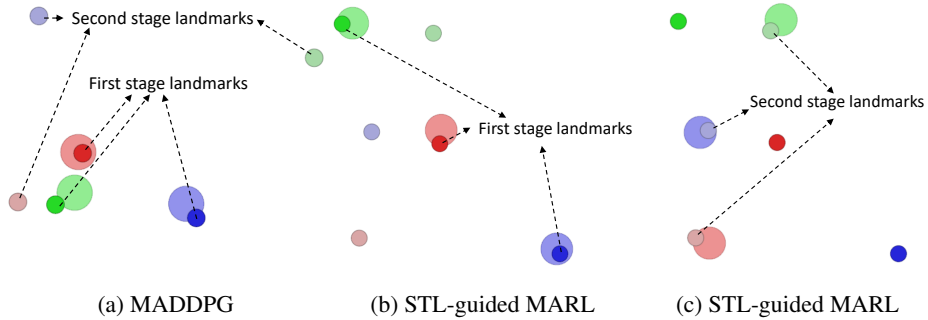


Figure 6: Simple coordination II in MPE. Agents trained with MADDPG algorithm hover around the first stage landmarks and fail to cover the second stage as shown in (a). Agents trained with STL-guided MARL visit the first stage landmarks and then covers the second stage landmarks as shown in (b) and (c).

In CARLA testbed, original reward for baseline algorithms is the weighted sum of speed reward r_i^{speed} , collision penalty $r_i^{\text{collision}}$ and dest reward r_i^{dest} , the weights for them and the constant in r_i^{dest} is: $w_1 = 1, w_2 = 1, w_3 = 0.5, c = 10$. For the STL reward $r_i^t = \sum_j c_j \rho(\varphi_{ij}, \omega, t) + b$, the weight corresponds to the STL specifications and the constant are set as: $c_1 = 5, c_2 = 1, c_3 = 5, c_4 = 5, b = 15$. The hyperparameters used for STL-guided MARL and baseline MAPPO algorithms is shown in Table 4. We use Fig. 7 to further illustrate the effectiveness of the STL-guided MARL algorithm with the screenshot figures of the testing process of different algorithms.

Table 4: Common hyperparameters for STL-guided MARL, MAPPO in CARLA testbed

Hyperparameter	Value
actor learning rate	7e-4
critic learning	7e-4
value loss	huber loss
critic loss	mse loss
Discount Factor	0.99
Batch Size	64
partial trajectory length	10
batch size	300
buffer length	300
optimizer	Adam
RNN hidden state dim	64
fc layer dim	64
activation layer	ReLU
use reward normalization	True
use feature normalization	True

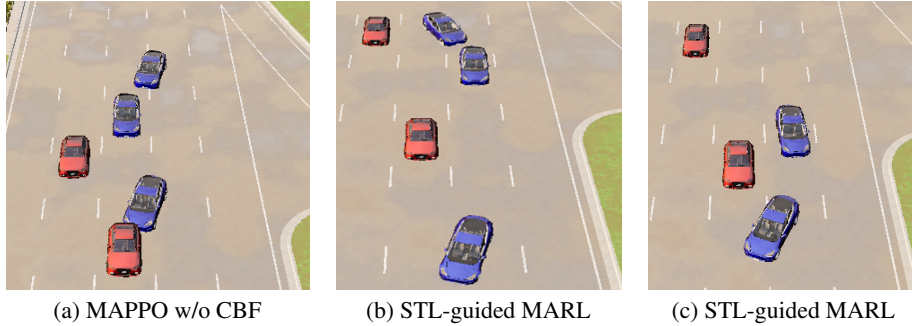


Figure 7: *Traffic-jam* scenario testing process in CARLA. Agents trained with the baseline algorithm fail to bypass the broken-down vehicle and collides with it as shown in (a). Agents trained with STL-guided MARL successfully pass through the only open lane without collision in a timely manner as shown in (b) and (c).

A.7 More Experiment Results

In order to further validate our proposed algorithm, We create a challenging scenario in CARLA called *Bottleneck* as shown in Fig 8. In this scenario, we spread more vehicles in all of the three lanes, while two lanes are being blocked by the broken-down vehicles. All the vehicles are required to bypass the two broken-down vehicles through the only open lane. For the baseline algorithms, MAPPO[20], MAPPO without STL-CBF safety shield, the reward function is same as in the *traffic-Jam* scenario. While for the STL-guided MARL, the STL specifications are same as in Eq. 5, the STL reward is the weighted sum of the robustness values given the STL specifications, $r_i^t = \sum_j c_j \rho(\varphi_{ij}, \omega, t) + b$, where c_j are weights and



Figure 8: *Bottleneck* in CARLA

b is a constant. We train the all the algorithms for 50 episodes with the episode length of 300 steps. The training results, including the mean episode return and the standard deviation for four agents are shown in Table 5. The safety rate is shown in Table 6. It can be seen that: (1) in *Bottleneck* scenario, STL-guided MARL achieves the best overall performance in terms of the mean episode return, demonstrating its capability of enable the agents learn a better policy to fulfill the STL specifications; (2) The algorithms with STL-CBF safety shield largely outperforms the baseline algorithm without it in terms of the safety rate. This shows the effectiveness of out proposed STL-CBF safety shield in providing safe guarantees for the system.

Table 5: Mean episode return in *Bottleneck* scenario.

Methods	Mean episode return			
	Agent 1	Agent 2	Agent 3	Agent 4
STL-guided MARL	6289.24 \pm 956.70	3410.89 \pm 1106.91	5152.67 \pm 900.39	6807.03 \pm 204.84
MAPPO	6149.78 \pm 965.51	3351.34 \pm 826.33	4556.96 \pm 1251.97	2928.52 \pm 2490.29
MAA2C	6362.12 \pm 458.74	3018.75 \pm 1067.15	5085.43 \pm 349.19	6794.62 \pm 264.87
MAPPO w/o CBF	5919.85 \pm 2037.28	3251.77 \pm 955.22	-1084.72 \pm 2536.89	3480.19 \pm 3488.49

Table 6: Safety rate in *Bottleneck* scenario

Methods	Safety rate
STL-guided MARL	98%
MAPPO	94%
MAA2C	98%
MAPPO w/o CBF	10%

A.8 Ablation study

A.8.1 Partial trajectory length

In order to investigate the influence of the partial trajectory length (L in Alg. 1) to the performance of STL-guided MARL algorithm, we use the *bottleneck* scenario in CARLA to test the performance given different partial trajectory lengths. We train the STL-guided MARL with different partial trajectory lengths for 50 episodes, with episode length of 300 steps, the training results are shown in Table 7. It can be observed that, when the partial trajectory length is 10, the STL-guided MARL shows the best performance in terms of mean episode return. When the partial trajectory length is too long, it is harder for the agent to correctly assign the credit to specific actions, and estimating the value function also becomes more challenging with longer future horizons. This may lead to the performance drop for the longer partial trajectory length. When the partial trajectory is very short, the agent’s experience and updates are based on a very limited number of steps, which may not be sufficient to effectively capture and exploit the long-term dependencies between the actions taken at each step and the objective task, e.g. the temporal requirement in STL specifications. This could be the reason for the performance drop for a short partial trajectory length.

Table 7: Mean episode return in *Bottleneck* scenario given different partial trajectory length. Selecting Partial trajectory length as 10 shows the best performance.

Partial trajectory length	Mean episode return			
	Agent 1	Agent 2	Agent 3	Agent 4
1	4599.98 \pm 633.38	2596.05 \pm 2003.17	3332.36 \pm 351.07	5228.03 \pm 255.82
10	6089.24 \pm 956.70	3410.89 \pm 1106.91	5152.67 \pm 900.39	6507.03 \pm 204.84
50	5683.18 \pm 1017.78	-1001.71 \pm 5047.77	4083.16 \pm 1323.32	6085.39 \pm 588.99

A.8.2 Temporal requirements

In order to evaluate the performance of STL-guided MARL in tasks with different types of temporal requirements, we consider the scenarios of simple coordination and simple spread in the MPE testbed, two tasks that temporal requirements of reaching the goals are not explicitly defined. Different from simple coordination II and simple spread II, these two tasks only have one stage of landmarks to reach. The reward used for baseline algorithm in simple coordination is $r = -\sum_{i=1}^N (|\mathbf{p}_i - \mathbf{p}_{i,\text{landmark}}|)$: where \mathbf{p}_i is location of agent i , $\mathbf{p}_{i,\text{landmark}}$ is location of the goal landmark of agent i , The reward

used for baseline algorithm in simple spread is $r = -\sum_{i=1}^N (\min_{j \in N} |\mathbf{p}_j - \mathbf{p}_{i,\text{landmark}}|)$, where \mathbf{p}_j is location of agent j , $\mathbf{p}_{i,\text{landmark}}$ is location of the landmark i . In both tasks, for a collision, there will be a -1 penalty added on the current reward. For the STL-guided MARL, the STL specifications in simple coordination is :

$$\varphi_{i_1} = \Diamond_{[0,T]} \bigwedge_{1,2,\dots} |\mathbf{p}_i^t - \mathbf{p}_{i,\text{landmark}}| \leq \epsilon_1, \quad (15)$$

Similarly, the STL specifications in simple spread II is:

$$\varphi_{i_1} = \Diamond_{[0,T]} \bigwedge_{1,2,\dots} \min_{j \in N} |\mathbf{p}_j^t - \mathbf{p}_{i,\text{landmark}}| \leq \epsilon_1, \quad (16)$$

The common safety requirement is: $\varphi_{i_2} = \Box_{[0,T]} \bigwedge_{1,2,\dots} |\mathbf{p}_i^t - \mathbf{p}_j^t| \geq D_{\text{safe}}, \forall j \in N$. the STL reward $r_i^t = \sum_j c_j \rho(\varphi_{i_j}, \omega, t) + b$, we set the weight for STL specifications and the constant as: $c_1 = 1, c_2 = 1, b = 0$.

We train the algorithms for 30000 episodes with episode length of 25. The training results are shown in Fig. 9 and Table 8. It can be observed that STL-guided MARL still shows better performance in both of the tasks. Compared with the performance in simple coordination II and simple spread II, the advantage of STL-guided MARL (compared with the baseline MARL such as MADDPG) becomes smaller. This illustrates that The STL-guided MARL can show more advantages when there are more temporal requirements in the tasks. With explicit requirements about the dynamic process of finishing some tasks or reaching some goals, STL specifications can also provide more information through the robustness value-based reward in the policy training process.

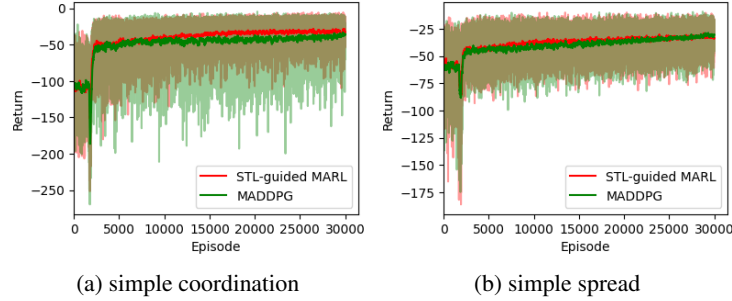


Figure 9: Training results in MPE.

Table 8: Mean episode return in MPE.

Methods	Simple coordination	Simple spread
STL-guided MARL	-42.59 ± 25.22	-38.40 ± 13.73
MADDPG	-49.12 ± 28.91	-40.26 ± 14.31